 CMES, vol.53, no.2, pp.117-145, 2009

Large Deformation Analyses of Space-Frame Structures, with Members of arbitrary Cross-Section, Using Explicit Tangent Stiffness Matrices, Based on a von Karman Type Nonlinear Theory in Rotated Reference Frames

Yongchang Cai[1,2], J.K. Paik[3] and Satya N. Atluri[3]

Abstract: This paper presents a simple finite element method, based on simple mechanics and physical clarity, for geometrically nonlinear large rotation analyses of space frames consisting of members of arbitrary cross-section. A co-rotational reference frame, involving the axes of each finitely rotated beam finite-element, is used as the Updated Lagrangian reference frame for the respective element. A von Karman type nonlinear theory of deformation is employed in the co-rotational reference frame of each beam element, to account for bending, stretching, and torsion of each element. An assumed displacement approach is used to derive an explicit expression for the (12x12) *symmetric* tangent stiffness matrix of the beam element in the co-rotational reference frame. From the finite-displacement vector at each of the two nodes of the beam element, an explicit expression is derived for the matrix of finite rotation of the co-rotational reference frame from the globally-fixed Cartesian reference frame. Thus, this paper provides a text-book example of an explicit expression for the (12x12) *symmetric tangent stiffness matrix* of a finitely deforming beam element, which can be employed in very simple analyses of large deformations of space-frames. This paper is also a celebration of the genius of Theodore von Karman (original Hungarian name Szöllöskislaki Kármán Tódor) (1881-1963), who received the first U.S. National Medal of Science in 1963, and who first proposed a simple nonlinear theory of plates in 1910, the essential ideas of which theory are adopted in the present paper, for beams of arbitrary cross-sections, in co-rotational reference frames. The present methodologies can be extended to study the very large deformations of plates and shells as well. Metal plasticity may

[1] Key Laboratory of Geotechnical and Underground Engineering of Ministry of Education, Department of Geotechnical Engineering, Tongji University, Shanghai 200092, P.R.China. E-mail: yc_cai@163.net

[2] Center for Aerospace Research & Education, University of California, Irvine

[3] Lloyd's Register Educational Trust (LRET) Center of Excellence, Pusan National University, Korea

also be included, through the method of plastic hinges, etc.

Keywords: Large deformation, Unsymmetrical cross-section, Explicit tangent stiffness, Updated Lagrangian formulation, Co-rotational reference frame, Rod, Space frames

1 Introduction

In the past decades, large deformation analyses of space frames have attracted much attention due to their significance in diverse engineering applications. Many different methods were developed by numerous researchers for the geometrically nonlinear analyses of 3D frame structures. Bathe and Bolourchi (1979) employed the total Lagrangian and updated Lagrangian approaches to formulate fully nonlinear 3D continuum beam elements. Punch and Atluri (1984) examined the performance of linear and quadratic Serendipity hybrid-stress 2D and 3D beam elements. Based on geometric considerations, Lo (1992) developed a general 3D nonlinear beam element, which can remove the restriction of small nodal rotations between two successive load increments. Kondoh, Tanaka and Atluri (1986), Kondoh and Atluri (1987), Shi and Atluri(1988) presented the derivations of explicit expressions of the tangent stiffness matrix, without employing either numerical or symbolic integration. Zhou and Chan (2004a, 2004b) developed a precise element capable of modeling elastoplastic buckling of a column by using a single element per member for large deflection analysis. Izzuddin (2001) clarified some of the conceptual issues which are related to the geometrically nonlinear analysis of 3D framed structures. Simo (1985), Mata, Oller and Barbat (2007, 2008), Auricchio, Carotenuto and Reali (2008) considered the nonlinear constitutive behavior in the geometrically nonlinear formulation for beams. Iura and Atluri (1988), Chan (1994), Xue and Meek (2001), Wu, Tsai and Lee(2009) studied the nonlinear dynamic response of the 3D frames. Lee, Lin, Lee, Lu and Liu (2008), Lee, Lu, Liu and Huang (2008) gave the exact large deflection solutions of the beams for some special cases. Dinis, Jorge and Belinha (2009), Han, Rajendran and Atluri (2005), Lee and Chen (2009) applied meshless methods to the analyses of nonlinear problems with large deformations or rotations. Large rotations in beams, plates and shells, and attendant variational principles involving the rotation tensor as a direct variable, were studied extensively by Atluri and his co-workers (see, for instance, Atluri (1980), Atluri(1984),and Atluri and Cazzani (1995)).

It is important to point out that, except for a few papers [Gendy and Saleeb (1992); Atluri, Iura, and Vasudevan(2001)] which have brief discussions of arbitrary cross sections, most of the studies were restricted to frames consisting of members with only symmetric cross sections. In practical engineering applications, such as in

stiffened plates (Fig.1), etc, beams of asymmetric or arbitrary cross sections play an important role and need to be considered.

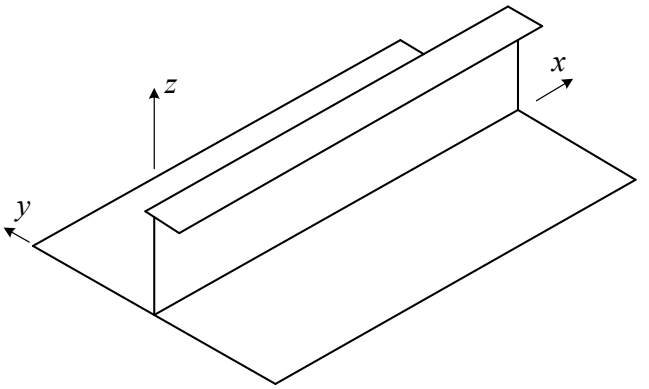

Figure 1: An example of stiffened plate

This paper presents a simple finite element method, based on simple mechanics and physical clarity, for geometrically nonlinear large rotation analyses of space frames consisting of members of arbitrary cross-section. A corotational-reference frame, involving the axes of each finitely rotated beam finite-element, is used as the Updated Lagrangian reference frame for the respective element. A von Karman type nonlinear theory of deformation is employed in the co-rotational reference frame of each beam element, to account for bending, stretching, and torsion of each element. An assumed displacement approach is used to derive an explicit expression for the (12x12) *symmetric* tangent stiffness matrix of the beam element in the co-rotational reference frame. From the finite-displacement vector at each of the two nodes of the beam element, an explicit expression is derived for the matrix of finite rotation of the co-rotational reference frame from the globally-fixed Cartesian reference frame. Thus, this paper provides a text-book example of an explicit expression for the (12x12) *symmetric tangent stiffness matrix* of a finitely deforming beam element, which can be employed in very simple analyses of large deformations of space-frames. This paper is also a celebration of the genius of Theodore von Karman (1881-1963), who received the first U.S. National Medal of Science in 1963, and who first proposed a simple nonlinear theory of plates in 1910, the essential ideas of which theory are adopted in the present paper, for beams of arbitrary cross-sections, in co-rotational reference frames. The present methodologies can be extended to study the very large deformations of plates and shells as well. Metal plasticity may also be included, through the method of plastic hinges, etc.

The present beam element has a much simpler form than those based on exact continuum theories of Simo (1985) and Bathe and Bolourchi (1979), but the accuracy of the present solutions for finite rotations is comparable to those in Simo (1985) and Bathe and Bolourchi (1979). The present explicit derivation of the tangent stiffness matrix of a finitely deforming beam of an arbitrary cross-section is more general and much simpler than in the earlier papers of Kondon, Tanaka and Atluri (1986), Kondoh and Atluri (1987), and Shi and Atluri (1988). Furthermore, unlike in the formulations of Simo(1985), Crisfield (1990) [and many others who followed them], which lead to currently popular myth that the stiffness matrices of finitely rotated structural members should be *unsymmetric*, the (12x12) stiffness matrix of the beam element in the present paper is enormously simple, and remains *symmetric* throughout the finite rotational deformation.

2 Von-Karman type nonlinear theory for a rod with large deformations

We consider a fixed global reference frame with axes $\bar{x}_i\,(i=1,2,3)$ and base vectors $\bar{\mathbf{e}}_i$. An initially straight rod of an arbitrary cross-section and base vectors $\tilde{\mathbf{e}}_i$, in its undeformed state, with local coordinates $\tilde{x}_i\,(i=1,2,3)$, is located arbitrarily in space, as shown in Fig.2. The current configuration of the rod, after arbitrarily large deformations (but small strains) is also shown in Fig.2.

The local coordinates in the reference frame in the current configuration are x_i and the base vectors are $\mathbf{e}_i\,(i=1,2,3)$. The nodes 1 and 2 of the rod (or an element of the rod) are supposed to undergo arbitrarily large displacements, and the rotations between the $\tilde{\mathbf{e}}_i\,(i=1,2,3)$ and the $\mathbf{e}_k\,(k=1,2,3)$ base vectors are assumed to be arbitrarily finite. In the continuing deformation from the current configuration, the local displacements in the $x_i\,(\mathbf{e}_i)$ coordinate system are assumed to be moderate, and the local gradient $(\partial u_{10}/\partial x_1)$ is assumed to be small compared to the transverse rotations $(\partial u_{\alpha 0}/\partial x_1)\,(\alpha=2,3)$. Thus, in essence, a von-Karman type deformation is assumed for the continued deformation from the current configuration, in the co-rotational frame of reference $\mathbf{e}_i\,(i=1,2,3)$ in the local coordinates $x_i\,(i=1,2,3)$. If H is the characteristic dimension of the cross-section of the rod, the precise assumptions governing the continued deformations from the current configuration are

$$\frac{u_{10}}{H} << 1; \frac{H}{L} << 1$$

$$\frac{u_{\alpha 0}}{H} \approx \mathrm{O}\,(1)\,(\alpha = 2,3)$$

$$\frac{\partial u_{10}}{\partial x_1} << \frac{\partial u_{\alpha 0}}{\partial x_1} \, (\alpha = 2,3)$$

and $\left(\frac{\partial u_{\alpha 0}}{\partial x_1}\right)^2 (\alpha = 2,3)$ are not negligible.

As shown in Fig.3, we consider the large deformations of a cylindrical rod, subjected to bending (in two directions), and torsion around x_1. The cross-section is unsymmetrical around x_2 and x_3 axes,and is constant along x_1.

As shown in Fig.3, the warping displacement due to the torque T around x_1 axis is $u_{1T}(x_2,x_3)$ and does not depend on x_1, the axial displacement at the origin ($x_2 = x_3 = 0$) is $u_{10}(x_1)$, and the bending displacement at $x_2 = x_3 = 0$ along the axis x_1 are $u_{20}(x_1)$ (along x_2) and $u_{30}(x_1)$ (along x_3).

We consider only loading situations when the generally 3-dimensional displacement state in the $\mathbf{e}_i$ system, donated as

$$u_i = u_i(x_k) \quad i = 1,2,3; \, k = 1,2,3$$

is simplified to be of the type:

$$\begin{aligned} u_1 &= u_{1T}(x_2,x_3) + u_{10}(x_1) - x_2 \frac{\partial u_{20}}{\partial x_1} - x_3 \frac{\partial u_{30}}{\partial x_1} \\ u_2 &= u_{20}(x_1) - \hat{\theta} x_3 \\ u_3 &= u_{30}(x_1) + \hat{\theta} x_2 \end{aligned} \tag{1}$$

where $\hat{\theta}$ is the total torsion of the rod at x_1 due to the torque T.

2.1 Strain-displacement relations

Considering only von Karman type nonlinearities in the rotated reference frame $\mathbf{e}_i(x_i)$, we can write the Green-Lagrange strain-displacement relations in the updated Lagrangian co-rotational frame $\mathbf{e}_i$ in Fig.2 as:

$$\begin{aligned} \varepsilon_{11} &= \frac{\partial u_1}{\partial x_1} + \frac{1}{2}\left(\frac{\partial u_2}{\partial x_1}\right)^2 + \frac{1}{2}\left(\frac{\partial u_3}{\partial x_1}\right)^2 \\ &= \frac{\partial u_{10}}{\partial x_1} + \frac{1}{2}\left(\frac{\partial u_{20}}{\partial x_1}\right)^2 + \frac{1}{2}\left(\frac{\partial u_{30}}{\partial x_1}\right)^2 - x_2 \frac{\partial^2 u_{20}}{\partial x_1^2} - x_3 \frac{\partial^2 u_{30}}{\partial x_1^2} \\ \varepsilon_{12} &= \frac{1}{2}\left(\frac{\partial u_1}{\partial x_2} + \frac{\partial u_2}{\partial x_1}\right) \\ &= \frac{1}{2}\left(\frac{\partial u_{1T}}{\partial x_2} - \frac{\partial u_{20}}{\partial x_1} + \frac{\partial u_{20}}{\partial x_1} - \frac{\partial \hat{\theta}}{\partial x_1} x_3\right) = \frac{1}{2}\left(\frac{\partial u_{1T}}{\partial x_2} - \theta \, x_3\right) \end{aligned}$$

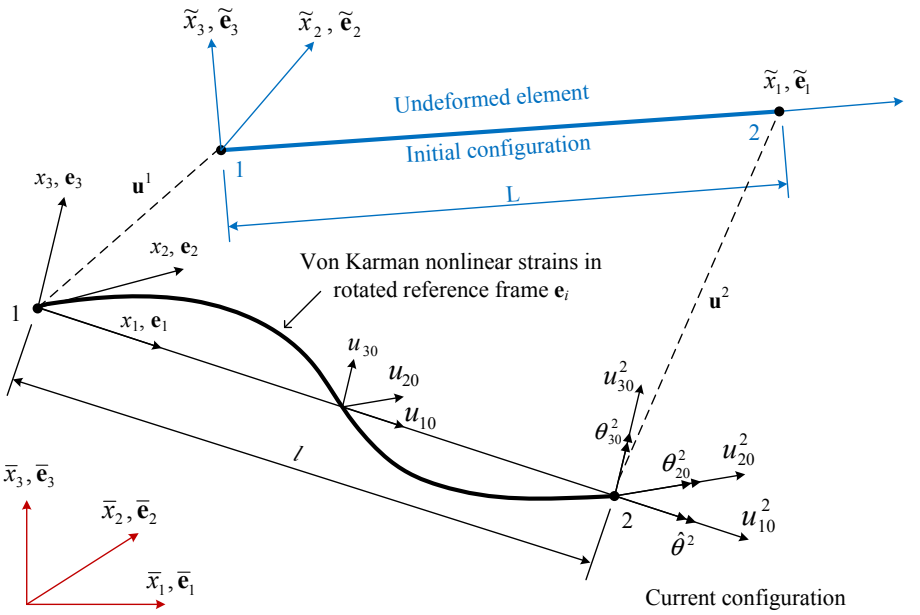

Figure 2: Kinematics of deformation of a space framed member

$$\begin{aligned}\varepsilon_{13} &= \frac{1}{2}\left(\frac{\partial u_1}{\partial x_3}+\frac{\partial u_3}{\partial x_1}\right)\\ &= \frac{1}{2}\left(\frac{\partial u_{1T}}{\partial x_3}-\frac{\partial u_{30}}{\partial x_1}+\frac{\partial u_{30}}{\partial x_1}+\theta x_2\right)=\frac{1}{2}\left(\frac{\partial u_{1T}}{\partial x_3}+\theta x_2\right)\end{aligned}$$

$$\begin{aligned}\varepsilon_{22} &= \frac{\partial u_2}{\partial x_2}+\frac{1}{2}\left(\frac{\partial u_1}{\partial x_2}\right)^2+\frac{1}{2}\left(\frac{\partial u_2}{\partial x_2}\right)^2+\frac{1}{2}\left(\frac{\partial u_3}{\partial x_2}\right)^2\\ &\approx 0+\frac{1}{2}\left(\frac{\partial u_{20}}{\partial x_1}\right)^2+0\approx 0\end{aligned} \tag{2}$$

$$\varepsilon_{23}\approx 0$$

$$\varepsilon_{33}\approx 0$$

where $\theta = d\hat{\theta}/dx_1$.

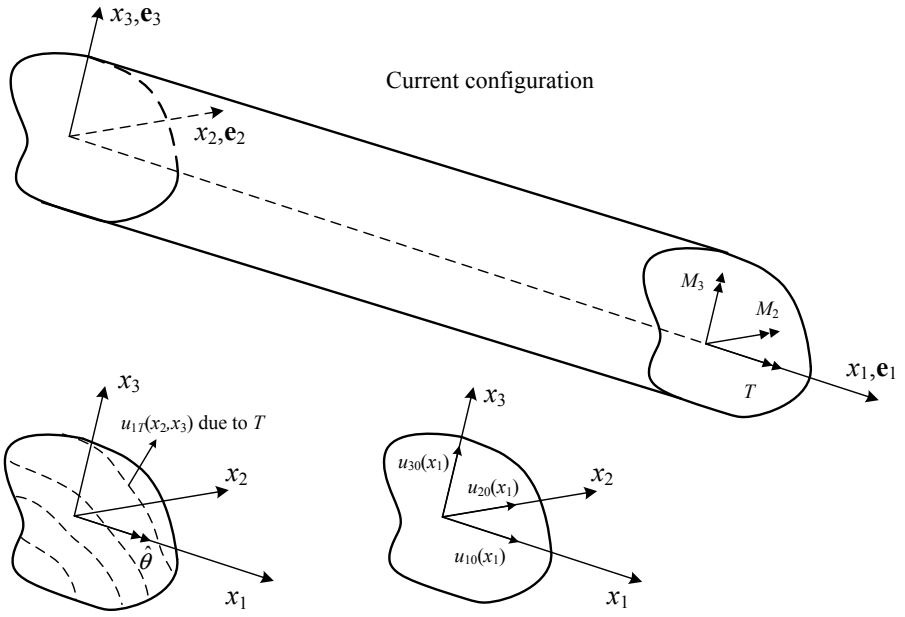

Figure 3: Large deformation analysis model of a cylindrical rod

By letting

$$\begin{aligned}
\chi_{22} &= -u_{20,11} \\
\chi_{33} &= -u_{30,11} \\
\varepsilon_{11}^0 &= u_{10,1} + \frac{1}{2}(u_{20,1})^2 + \frac{1}{2}(u_{30,1})^2 \\
&= \varepsilon_{11}^{0\mathrm{L}} + \varepsilon_{11}^{0\mathrm{NL}}
\end{aligned} \tag{3}$$

the strain-displacement relations can be rewritten as

$$\begin{aligned}
\varepsilon_{11} &= \varepsilon_{11}^0 + x_2\chi_{22} + x_3\chi_{33} \\
\varepsilon_{12} &= \frac{1}{2}(u_{1T,2} - \theta x_3) \\
\varepsilon_{13} &= \frac{1}{2}(u_{1T,3} + \theta x_2) \\
\varepsilon_{22} &= \varepsilon_{33} = \varepsilon_{23} = 0
\end{aligned} \tag{4}$$

where $,i$ denotes a differentiation with respect to x_i.

The matrix form of the Eq.(4) is

$$\boldsymbol{\varepsilon} = \boldsymbol{\varepsilon}^L + \varepsilon^N \tag{5}$$

where

$$\boldsymbol{\varepsilon}^L = \begin{Bmatrix} \varepsilon_{11}^L \\ \varepsilon_{12}^L \\ \varepsilon_{13}^L \end{Bmatrix} = \begin{Bmatrix} u_{10,1} + x_2\chi_{22} + x_3\chi_{33} \\ \frac{1}{2}\left(u_{1T,2} - \theta x_3\right) \\ \frac{1}{2}\left(u_{1T,3} + \theta x_2\right) \end{Bmatrix} \tag{6}$$

$$\boldsymbol{\varepsilon}^N = \begin{Bmatrix} \varepsilon_{11}^N \\ \varepsilon_{12}^N \\ \varepsilon_{13}^N \end{Bmatrix} = \begin{Bmatrix} \frac{1}{2}\left(u_{20,1}\right)^2 + \frac{1}{2}\left(u_{30,1}\right)^2 \\ 0 \\ 0 \end{Bmatrix} \tag{7}$$

2.2 Stress-Strain relations

Taking the material to be linear elastic, we assume that the additional second Piola-Kirchhoff stress, denoted by tensor $\mathbf{S}^1$ in the updated Lagrangian co-rotational reference frame $\mathbf{e}_i$ of Fig.2 (in addition to the pre-existing Cauchy stress due to prior deformation, denoted by τ^0), is given by:

$$\begin{aligned} S_{11}^1 &= E\varepsilon_{11} \\ S_{12}^1 &= 2\mu\varepsilon_{12} \\ S_{13}^1 &= 2\mu\varepsilon_{13} \\ S_{22}^1 &= S_{33}^1 = S_{23}^1 \approx 0 \end{aligned} \tag{8}$$

where $\mu = \frac{E}{2(1+\nu)}$; E is the elastic modulus; ν is the Poisson ratio.
By using Eq.(5), Eq.(8) can also be written as

$$\mathbf{S}^1 = \tilde{\mathbf{D}}\left(\boldsymbol{\varepsilon}^L + \boldsymbol{\varepsilon}^N\right) = \mathbf{S}^{1L} + \mathbf{S}^{1N} \tag{9}$$

where

$$\tilde{\mathbf{D}} = \begin{bmatrix} E & 0 & 0 \\ 0 & 2\mu & 0 \\ 0 & 0 & 2\mu \end{bmatrix} \tag{10}$$

From Eq.(4) and Eq.(8), the generalized nodal forces of the rod element in Fig.3

can be written as

$$
\begin{aligned}
N_{11} &= \int_A S_{11}^1 dA = E\left(A\varepsilon_{11}^0 + \chi_{22}\int_A x_2 dA + \chi_{33}\int_A x_3 dA\right) \\
&= E\left(A\varepsilon_{11}^0 + I_2\chi_{22} + I_3\chi_{33}\right) \\
M_{33} &= \int_A S_{11}^1 x_3 dA = E\int_A \left(A\varepsilon_{11}^0 + x_2\chi_{22} + x_3\chi_{33}\right)x_3 dA \\
&= E\left(I_3\varepsilon_{11}^0 + I_{23}\chi_{22} + I_{33}\chi_{33}\right) \\
M_{22} &= \int_A S_{11}^1 x_2 dA = E\int_A \left(A\varepsilon_{11}^0 + x_2\chi_{22} + x_3\chi_{33}\right)x_2 dA \\
&= E\left(I_2\varepsilon_{11}^0 + I_{22}\chi_{22} + I_{23}\chi_{33}\right) \\
T &= \int_A S_{13}^1 x_2 - S_{12}^1 x_3 dA = 2\mu\int_A \left(x_2\varepsilon_{13} + x_3\varepsilon_{12}\right)x_2 dA \\
&= \frac{2\mu}{2}\int_A \left[\left(u_{1T,3} + \theta\, x_2\right)x_2 - \left(u_{1T,2} - \theta x_3\right)\right]dA \\
&= \mu\int_A \theta\left(x_2^2 + x_3^2\right)dA + \mu\int_A \left(u_{1T,3}x_2 - u_{1T,2}x_3\right)dA \\
&= \mu I_{rr}\theta + \mu\int_S \left(u_{1T}n_3x_2 - u_{1T}n_2x_3\right)dS \\
&= \mu I_{rr}\theta
\end{aligned}
\tag{11}
$$

where n_j is the outward norm, $I_2 = \int_A x_2 dA, I_3 = \int_A x_3 dA, I_{22} = \int_A x_2^2 dA, I_{33} = \int_A x_3^2 dA$, $I_{23} = \int_A x_2 x_3 dA$, and $I_{rr} = \int_A \left(x_2^2 + x_3^2\right) dA$.
The matrix form of the above equations is

$$
\begin{Bmatrix} \sigma_1 \\ \sigma_2 \\ \sigma_3 \\ \sigma_4 \end{Bmatrix} = \begin{Bmatrix} N_{11} \\ M_{22} \\ M_{33} \\ T \end{Bmatrix} = \begin{bmatrix} EA & EI_2 & EI_3 & 0 \\ EI_2 & EI_{22} & EI_{23} & 0 \\ EI_3 & EI_{23} & EI_{33} & 0 \\ 0 & 0 & 0 & \mu I_{rr} \end{bmatrix} \begin{Bmatrix} \varepsilon_{11}^0 \\ \chi_{22} \\ \chi_{33} \\ \theta \end{Bmatrix} \tag{12}
$$

It can be denoted as

$$
\boldsymbol{\sigma} = \mathbf{DE} \tag{13}
$$

where

$$
\boldsymbol{\sigma} = \begin{Bmatrix} \sigma_1 \\ \sigma_2 \\ \sigma_3 \\ \sigma_4 \end{Bmatrix} = \begin{Bmatrix} N_{11} \\ M_{22} \\ M_{33} \\ T \end{Bmatrix} = \text{element generalized stresses} \tag{14}
$$

$$\mathbf{D} = \begin{bmatrix} EA & EI_2 & EI_3 & 0 \\ EI_2 & EI_{22} & EI_{23} & 0 \\ EI_3 & EI_{23} & EI_{33} & 0 \\ 0 & 0 & 0 & \mu I_{rr} \end{bmatrix} \tag{15}$$

$$\mathbf{E} = \begin{Bmatrix} E_1 \\ E_2 \\ E_3 \\ E_4 \end{Bmatrix} = \begin{Bmatrix} \varepsilon_{11}^0 \\ \chi_{22} \\ \chi_{33} \\ \theta \end{Bmatrix} = \text{element generalized strains} \tag{16}$$

By letting

$$\mathbf{U} = \begin{Bmatrix} \hat{u}_1 \\ \hat{u}_2 \\ \hat{u}_3 \\ \hat{u}_4 \end{Bmatrix} = \begin{Bmatrix} u_{10} \\ u_{20} \\ u_{30} \\ \hat{\theta} \end{Bmatrix} \tag{17}$$

Eq.(16) can be written as

$$\mathbf{E} = \mathbf{E}^L + \mathbf{E}^N = \mathbf{LU} + \frac{1}{2}\mathbf{AHU} \tag{18}$$

where $\mathbf{E}^L = \mathbf{LU}$, $\mathbf{E}^N = \frac{1}{2}\mathbf{AHU}$,

$$\mathbf{L} = \begin{bmatrix} \frac{\partial}{\partial x_1} & 0 & 0 & 0 \\ 0 & -\frac{\partial^2}{\partial x_1^2} & 0 & 0 \\ 0 & 0 & -\frac{\partial^2}{\partial x_1^2} & 0 \\ 0 & 0 & 0 & \frac{\partial}{\partial x_1} \end{bmatrix} \tag{19}$$

$$\mathbf{A} = \begin{bmatrix} 0 & \frac{\partial \hat{u}_2}{\partial x_1} & \frac{\partial \hat{u}_3}{\partial x_1} & 0 \\ 0 & 0 & 0 & 0 \\ 0 & 0 & 0 & 0 \\ 0 & 0 & 0 & 0 \end{bmatrix} \tag{20}$$

$$\mathbf{H} = \begin{bmatrix} 0 & 0 & 0 & 0 \\ 0 & \frac{\partial}{\partial x_1} & 0 & 0 \\ 0 & 0 & \frac{\partial}{\partial x_1} & 0 \\ 0 & 0 & 0 & 0 \end{bmatrix} \tag{21}$$

By using Eq.(18), Eq.(13) can be rewritten as

$$\boldsymbol{\sigma} = \mathbf{DE}^L + \mathbf{DE}^N = \boldsymbol{\sigma}^L + \boldsymbol{\sigma}^N \tag{22}$$

3 Updated Lagrangian formulation in the co-rotational reference frame $\mathbf{e}_i$

3.1 Interpolation functions

As shown in Fig.2, the rod element has two nodes with 6 degrees of freedom per node. By defining the following shape functions

$$\phi_1 = 1-\xi, \phi_2 = \xi \tag{23}$$

$$\begin{aligned} &N_1 = 1-3\xi^2+2\xi^3, N_3 = 3\xi^2-2\xi^3 \\ &N_2 = \left(\xi-2\xi^2+\xi^3\right) l, N_4 = \left(\xi^3-\xi^2\right) l \end{aligned} \tag{24}$$

where l is the length of the rod element,

$$\xi = \frac{x_1 - x_1^1}{l} \, (0 < \xi < 1)$$

and x_1^1 is the coordinate of the node 1 along axis x_1, we can approximate the displacement function in each rod element by

$$\mathbf{U} = \mathbf{N}\hat{\mathbf{a}} = \begin{bmatrix} \mathbf{N}_1 & \mathbf{N}_2 \end{bmatrix} \begin{Bmatrix} \mathbf{u}^1 \\ \mathbf{u}^2 \end{Bmatrix} \tag{25}$$

where the displacement interpolation matrix is

$$\mathbf{N}_1 = \begin{bmatrix} \phi_1 & 0 & 0 & 0 & 0 & 0 \\ 0 & N_1 & 0 & 0 & 0 & N_2 \\ 0 & 0 & N_1 & 0 & -N_2 & 0 \\ 0 & 0 & 0 & \phi_1 & 0 & 0 \end{bmatrix} \tag{26}$$

$$\mathbf{N}_2 = \begin{bmatrix} \phi_2 & 0 & 0 & 0 & 0 & 0 \\ 0 & N_3 & 0 & 0 & 0 & N_4 \\ 0 & 0 & N_3 & 0 & -N_4 & 0 \\ 0 & 0 & 0 & \phi_2 & 0 & 0 \end{bmatrix} \tag{27}$$

and the displacement vectors of node i in the updated Lagrangian co-rotational frame $\mathbf{e}_i$ of Fig.2 are:

$$\mathbf{u}^i = \begin{bmatrix} u_1^i & u_2^i & u_3^i & u_4^i & u_5^i & u_6^i \end{bmatrix}^T = \begin{bmatrix} u_{10}^i & u_{20}^i & u_{30}^i & \hat{\theta}^i & \theta_{20}^i & \theta_{30}^i \end{bmatrix}^T \quad [i = 1,2] \tag{28}$$

From Eqs.(18) and (25), one can obtain

$$\mathbf{E} = \mathbf{E}^L + \mathbf{E}^N = \left(\mathbf{B}^L + \hat{\mathbf{B}}^N\right) \hat{\mathbf{a}} \tag{29}$$

where

$$\mathbf{B}^L = \left[\begin{array}{cccccc|cccccc} \frac{\partial \phi_1}{\partial x_1} & 0 & 0 & 0 & 0 & 0 & & & & & & \\ 0 & -\frac{\partial^2 N_1}{\partial x_1^2} & 0 & 0 & 0 & -\frac{\partial^2 N_2}{\partial x_1^2} & & & & & & \\ 0 & 0 & -\frac{\partial^2 N_1}{\partial x_1^2} & 0 & \frac{\partial^2 N_2}{\partial x_1^2} & 0 & & & & & & \\ 0 & 0 & 0 & \frac{\partial \phi_1}{\partial x_1} & 0 & 0 & & & & & & \end{array}\right.$$
$$\left.\begin{array}{cccccc} \frac{\partial \phi_2}{\partial x_1} & 0 & 0 & 0 & 0 & 0 \\ 0 & -\frac{\partial^2 N_3}{\partial x_1^2} & 0 & 0 & 0 & -\frac{\partial^2 N_4}{\partial x_1^2} \\ 0 & 0 & -\frac{\partial^2 N_3}{\partial x_1^2} & 0 & \frac{\partial^2 N_4}{\partial x_1^2} & 0 \\ 0 & 0 & 0 & \frac{\partial \phi_2}{\partial x_1} & 0 & 0 \end{array}\right] \tag{30}$$

$$\mathbf{G} = \mathbf{H}\mathbf{N} = \left[\begin{array}{cccccc|cccccc} 0 & 0 & 0 & 0 & 0 & 0 & & & & & & \\ 0 & \frac{\partial N_1}{\partial x_1} & 0 & 0 & 0 & \frac{\partial N_2}{\partial x_1} & & & & & & \\ 0 & 0 & \frac{\partial N_1}{\partial x_1} & 0 & -\frac{\partial N_2}{\partial x_1} & 0 & & & & & & \\ 0 & 0 & 0 & 0 & 0 & 0 & & & & & & \end{array}\right.$$
$$\left.\begin{array}{cccccc} 0 & 0 & 0 & 0 & 0 & 0 \\ 0 & \frac{\partial N_3}{\partial x_1} & 0 & 0 & 0 & \frac{\partial N_4}{\partial x_1} \\ 0 & 0 & \frac{\partial N_3}{\partial x_1} & 0 & -\frac{\partial N_4}{\partial x_1} & 0 \\ 0 & 0 & 0 & 0 & 0 & 0 \end{array}\right] \tag{31}$$

$$\hat{\mathbf{B}}^N == \frac{1}{2}\mathbf{A}\mathbf{G} = \left[\begin{array}{cccccc|cccccc} 0 & \frac{\partial N_1}{\partial x_1}\frac{\partial \hat{u}_2^k}{\partial x_1} & \frac{\partial N_1}{\partial x_1}\frac{\partial \hat{u}_3^k}{\partial x_1} & 0 & -\frac{\partial N_2}{\partial x_1}\frac{\partial \hat{u}_3^k}{\partial x_1} & \frac{\partial N_2}{\partial x_1}\frac{\partial \hat{u}_2^k}{\partial x_1} & & & & & & \\ 0 & 0 & 0 & 0 & 0 & 0 & & & & & & \\ 0 & 0 & 0 & 0 & 0 & 0 & & & & & & \\ 0 & 0 & 0 & 0 & 0 & 0 & & & & & & \end{array}\right.$$
$$\left.\begin{array}{cccccc} 0 & \frac{\partial N_3}{\partial x_1}\frac{\partial \hat{u}_2^k}{\partial x_1} & \frac{\partial N_3}{\partial x_1}\frac{\partial \hat{u}_3^k}{\partial x_1} & 0 & -\frac{\partial N_4}{\partial x_1}\frac{\partial \hat{u}_3^k}{\partial x_1} & \frac{\partial N_4}{\partial x_1}\frac{\partial \hat{u}_2^k}{\partial x_1} \\ 0 & 0 & 0 & 0 & 0 & 0 \\ 0 & 0 & 0 & 0 & 0 & 0 \\ 0 & 0 & 0 & 0 & 0 & 0 \end{array}\right] \tag{32}$$

and thus

$$\delta(\mathbf{E}) = \left(\mathbf{B}^L + 2\hat{\mathbf{B}}^N\right)\delta\hat{\mathbf{a}} = \left(\mathbf{B}^L + \mathbf{B}^N\right)\delta(\hat{\mathbf{a}}) = \mathbf{B}\delta\hat{\mathbf{a}} \tag{33}$$

3.2 Updated Lagrangian (U.L.), Assumed Dispacement, weak-formulation of the rod element in the co-rotational reference frame

If τ_{ij}^0 are the initial Cauchy stresses in the updated Lagrangian co-rotational frame $\mathbf{e}_i$ of Fig.2, and S_{ij}^1 are the additional (incremental) second Piola-Kirchhoff stresses in the same updated Lagrangian co-rotational frame with axes $\mathbf{e}_i$, then the static equations of linear momentum balance and the stress boundary conditions in the frame $\mathbf{e}_i$ are given by

$$\frac{\partial}{\partial x_i}\left[\left(S_{ik}^1+\tau_{ik}^0\right)\left(\delta_{jk}+\frac{\partial u_j}{\partial x_k}\right)\right]+b_j=0 \tag{34}$$

$$\left(S_{ik}^1+\tau_{ik}^0\right)\left(\delta_{jk}+\frac{\partial u_j}{\partial x_k}\right)n_i-f_j=0 \tag{35}$$

where b_j are the body forces per unit volume in the current reference state, and f_j are the given boundary loads.

By letting $S_{ik}=S_{ik}^1+\tau_{ik}^0$, the equivalent weak form of the above equations can be written as

$$\int_V\left\{\frac{\partial}{\partial x_i}\left[S_{ik}\left(\delta_{jk}+\frac{\partial u_j}{\partial x_k}\right)\right]+b_j\right\}\delta u_j dV - \int_{S_\sigma}\left[S_{ik}\left(\delta_{jk}+\frac{\partial u_j}{\partial x_k}\right)n_i-f_j\right]\delta u_j dS=0 \tag{36}$$

where δu_j are the test functions.

By integrating by parts the first item of the left side, the above equation can be written as

$$\int_V -S_{ik}\left(\delta_{jk}+\frac{\partial u_j}{\partial x_k}\right)\delta u_{j,i}dV+\int_V b_j\delta u_j dV+\int_{S_\sigma} f_j\delta u_j dS=0 \tag{37}$$

From Eq.(9) we may write

$$S_{ik}^1=S_{ik}^{1\mathrm{L}}+S_{ik}^{1\mathrm{N}} \tag{38}$$

Then the first item of Eq.(37) becomes

$$\begin{aligned}S_{ik}\left(\delta_{jk}+u_{j,k}\right)\delta u_{j,i}&=\left(\tau_{ij}^0+\tau_{ik}^0u_{j,k}+S_{ij}^{1\mathrm{L}}+S_{ij}^{1\mathrm{N}}+S_{ik}^1u_{j,k}\right)\delta u_{j,i}\\&=S_{ij}^{1\mathrm{L}}\delta\varepsilon_{ij}^L+\tau_{ik}^0\delta\left(\frac{1}{2}u_{j,k}u_{j,i}\right)+\left(\tau_{ij}^0+S_{ij}^{1\mathrm{N}}+S_{ik}^1u_{j,k}\right)\delta u_{j,i}\end{aligned} \tag{39}$$

By using Eq.(5), Eq.(37) may be written as

$$\int_V \left(S_{ij}^{1\mathrm{L}}\delta\varepsilon_{ij}^L+\tau_{ij}^0\delta\varepsilon_{ij}^N\right)dV= \int_V b_j\delta u_j dV+\int_{S_\sigma} f_j\delta u_j dS-\int_V\left(\tau_{ij}^0+S_{ij}^{1\mathrm{N}}+S_{ik}^1u_{j,k}\right)\delta\varepsilon_{ij}^L dV \quad (40)$$

The terms on the right hand side are 'correction' terms in a Newton-Rapson type iterative approach. Carrying out the integration over the cross sectional area of each rod, and using Eqs.(1) to (33), then Eq.(40) can be easily shown to reduce to:

$$\sum_e\left[\delta\hat{\mathbf{a}}^T\int_l\left(\mathbf{B}^L\right)^T\mathbf{D}\mathbf{B}^L dl\,\hat{\mathbf{a}}+\delta\hat{\mathbf{a}}^T\int_l\left(\mathbf{B}^N\right)^T\boldsymbol{\sigma}^0 dl\right]= \sum_e\left[\delta\hat{\mathbf{a}}^T\hat{\mathbf{F}}^1-\delta\hat{\mathbf{a}}^T\int_l\left(\mathbf{B}^L\right)^T\left(\boldsymbol{\sigma}^0+\mathbf{S}^{1N}\right)dl-\delta\hat{\mathbf{a}}^T\int_l\left(\mathbf{B}^N\right)^T\mathbf{S}^1 dl\right] \quad (41)$$

where $\hat{\mathbf{F}}^1=\int_V\mathbf{N}^T\mathbf{b}^* dV+\int_{S_\sigma}\mathbf{N}^T\mathbf{f}^* dS$ is the external equivalent nodal force.
Eq.(41) can be rewritten as

$$\sum_e\left[\delta\hat{\mathbf{a}}^T\left(\hat{\mathbf{K}}^L+\hat{\mathbf{K}}^S\right)\hat{\mathbf{a}}\right]=\sum_e\left[\delta\hat{\mathbf{a}}^T\left(\hat{\mathbf{F}}^1-\hat{\mathbf{F}}^S\right)\right] \quad (42)$$

where $\hat{\mathbf{K}}=\hat{\mathbf{K}}^L+\hat{\mathbf{K}}^S$ is the *symmetric tangent stiffness matrix* of the rod element,

$$\hat{\mathbf{K}}^L=\int_l\left(\mathbf{B}^L\right)^T\mathbf{D}\mathbf{B}^L dl \text{ linear part} \quad (43)$$

$$\hat{\mathbf{K}}^S=\int_l\left(\mathbf{B}^N\right)^T\boldsymbol{\sigma}^0 dl=\int_l\sigma_1^0\mathbf{G}^T\mathbf{G}dl \text{ nonlinear part} \quad (44)$$

and

$$\hat{\mathbf{F}}^S=\int_l\left(\mathbf{B}^L\right)^T\left(\boldsymbol{\sigma}^0+\sigma^{1N}\right)dl+\int_l\left(\mathbf{B}^N\right)^T\boldsymbol{\sigma}^1 dl=\int_0^1\mathbf{F}_\sigma(\xi)\,d\xi \quad (45)$$

where $\boldsymbol{\sigma}=\boldsymbol{\sigma}^0+\sigma^1=\boldsymbol{\sigma}^0+\boldsymbol{\sigma}^{1L}+\boldsymbol{\sigma}^{1N}$ are the element generalized stresses.

If we neglect the nonlinear items in Eq.(45) for the convenience of solving the nonlinear equation, and substituting Eq.(13) and Eq.(30) into Eq.(45), $\mathbf{F}_\sigma(\xi)$ can be written as

$$\mathbf{F}_\sigma(\xi) = \left[\begin{array}{cccccccccccc} -\sigma_1^0 & \frac{6-12\xi}{l}\sigma_2^0 & \frac{6-12\xi}{l}\sigma_3^0 & -\sigma_4^0 & (-4+6\xi)\sigma_3^0 & (4-6\xi)\sigma_2^0 \\ \sigma_1^0 & \frac{-6+12\xi}{l}\sigma_2^0 & \frac{-6+12\xi}{l}\sigma_3^0 & \sigma_4^0 & (6\xi-2)\sigma_3^0 & -(6\xi-2)\sigma_2^0 \end{array} \right]^T \tag{46}$$

3.3 Explicit expressions of the tangent stiffness matrix

We assume for simplicity that the initial stress state σ_1^0 is constant in a rod element. The components of the element tangent stiffness matrix, $\hat{\mathbf{K}}^L$ and $\hat{\mathbf{K}}^S$, respectively, can be derived explicitly, after some simple algebra, as follows.

$$\hat{\mathbf{K}}^S = \frac{\sigma_1^0}{l} \begin{bmatrix} 0 & 0 & 0 & 0 & 0 & 0 & 0 & 0 & 0 & 0 & 0 & 0 \\ & 1.2 & 0 & 0 & 0 & 0.1l & 0 & -1.2 & 0 & 0 & 0 & 0.1l \\ & & 1.2 & 0 & -0.1l & 0 & 0 & 0 & -1.2 & 0 & -0.1l & 0 \\ & & & 0 & 0 & 0 & 0 & 0 & 0 & 0 & 0 & 0 \\ & & & & \frac{2l^2}{15} & 0 & 0 & 0 & 0.1l & 0 & \frac{-l^2}{30} & 0 \\ & & & & & \frac{2l^2}{15} & 0 & -0.1l & 0 & 0 & 0 & \frac{-l^2}{30} \\ & & & & & & 0 & 0 & 0 & 0 & 0 & 0 \\ & & & & & & & 1.2 & 0 & 0 & 0 & -0.1l \\ & & & & & & & & 1.2 & 0 & 0.1l & 0 \\ & & & & & & & & & 0 & 0 & 0 \\ & & & & sym. & & & & & & \frac{2l^2}{15} & 0 \\ & & & & & & & & & & & \frac{2l^2}{15} \end{bmatrix}_{12\times 12} \tag{47}$$

The symmetric stiffness matrix $\hat{\mathbf{K}}^S(12\times 12)$, accounts for the interaction of the axial stress in the beam in the co-rotational reference frame, with the continued transverse displacement in the beam in the co-rotational reference frame. If the axial load in the beam is compressive, $\hat{\mathbf{K}}^S$ will account for the phenomenon of the buckling in the beam. In Eq.(47), l is the current length of the beam element in the current reference state with base vectors $\mathbf{e}_i$, as shown in Fig.2.

$$\hat{\mathbf{K}}^L = \frac{E}{l} \begin{bmatrix} \hat{\mathbf{K}}^{\mathrm{L1}} & \hat{\mathbf{K}}^{\mathrm{L12}} \\ \left(\hat{\mathbf{K}}^{\mathrm{L12}}\right)^T & \hat{\mathbf{K}}^{\mathrm{L2}} \end{bmatrix} \tag{48}$$

where

$$\hat{\mathbf{K}}^{\mathrm{L1}} = \begin{bmatrix} A & 0 & 0 & 0 & I_3 & -I_2 \\ & 12I_{22}/l^2 & 12I_{23}/l^2 & 0 & -6I_{23}/l & 6I_{22}/l \\ & & 12I_{33}/l^2 & 0 & -6I_{33}/l & 6I_{23}/l \\ & & & \frac{\mu}{E}I_{rr} & 0 & 0 \\ & \text{symmetric} & & & 4I_{33} & -4I_{23} \\ & & & & & 4I_{22} \end{bmatrix} \tag{49}$$

$$\hat{\mathbf{K}}^{L2} = \begin{bmatrix} A & 0 & 0 & 0 & I_3 & -I_2 \\ & 12I_{22}/l^2 & 12I_{23}/l^2 & 0 & 6I_{23}/l & -6I_{22}/l \\ & & 12I_{33}/l^2 & 0 & 6I_{33}/l & -6I_{23}/l \\ & & & \frac{\mu}{E}I_{rr} & 0 & 0 \\ & \text{symmetric} & & & 4I_{33} & -4I_{23} \\ & & & & & 4I_{22} \end{bmatrix} \tag{50}$$

$$\hat{\mathbf{K}}^{L12} = \begin{bmatrix} -A & 0 & 0 & 0 & -I_3 & I_2 \\ 0 & -12I_{22}/l^2 & -12I_{23}/l^2 & 0 & -6I_{23}/l & 6I_{22}/l \\ 0 & -12I_{23}/l^2 & -12I_{33}/l^2 & 0 & -6I_{33}/l & 6I_{23}/l \\ 0 & 0 & 0 & -\frac{\mu}{E}I_{rr} & 0 & 0 \\ -I_3 & 6I_{23}/l & 6I_{33}/l & 0 & 2I_{33} & -2I_{23} \\ I_2 & -6I_{22}/l & -6I_{23}/l & 0 & -2I_{23} & 2I_{22} \end{bmatrix} \tag{51}$$

Thus, $\hat{\mathbf{K}}^L$ is the usual linear symmetric (12×12) stiffness matrix of the beam in the co-rotational reference frame, with the geometric parameters $I_2, I_3, I_{22}, I_{33}, I_{23}$ and I_{rr}, and the current length l.

It is clear from the above procedures, that the present (12×12) symmetric tangent stiffness matrices of the beam in the co-rotational reference frame, based on the simplified rod theory, are much simpler than those based on the exact continuum beam theories of Simo (1985), and Bathe and Bolourchi (1979), or those of Kondon, Tanaka and Atluri (1986), Kondoh and Atluri (1987), and Shi and Atluri (1988). Moreover, the explicit expressions for the tangent stiffness matrix of each rod can be seen to be derived as text-book examples of nonlinear analyses.

4 Transformation between deformation dependent co-rotational local $[\mathbf{e}_i]$, and the global $[\bar{\mathbf{e}}_i]$ frames of reference

As shown in Fig.2, $\bar{x}_i\,(i=1,2,3)$ are the global coordinates with unit basis vectors $\bar{\mathbf{e}}_i$. $\tilde{x}_i$ and $\tilde{\mathbf{e}}_i$ are the local coordinates for the rod element at the undeformed element.

The basis vector $\tilde{\mathbf{e}}_i$ are initially chosen such that (Shi and Atluri 1988)

$$\begin{aligned}
\tilde{\mathbf{e}}_1 &= (\Delta\tilde{x}_1\bar{\mathbf{e}}_1 + \Delta\tilde{x}_2\bar{\mathbf{e}}_2 + \Delta\tilde{x}_3\bar{\mathbf{e}}_3)/L \\
\tilde{\mathbf{e}}_2 &= (\bar{\mathbf{e}}_3 \times \tilde{\mathbf{e}}_1)/|\bar{\mathbf{e}}_3 \times \tilde{\mathbf{e}}_1| \\
\tilde{\mathbf{e}}_3 &= \tilde{\mathbf{e}}_1 \times \tilde{\mathbf{e}}_2
\end{aligned} \tag{52}$$

where $\Delta\tilde{x}_i = \tilde{x}_i^2 - \tilde{x}_i^1, L = \left(\Delta\tilde{x}_1^2 + \Delta\tilde{x}_2^2 + \Delta\tilde{x}_3^2\right)^{\frac{1}{2}}$.
Then $\tilde{\mathbf{e}}_i$ and $\bar{\mathbf{e}}_i$ have the following relations:

$$\begin{Bmatrix} \tilde{\mathbf{e}}_1 \\ \tilde{\mathbf{e}}_2 \\ \tilde{\mathbf{e}}_3 \end{Bmatrix} = \begin{bmatrix} \Delta\tilde{x}_1/L & \Delta\tilde{x}_2/L & \Delta\tilde{x}_3/L \\ -\Delta\tilde{x}_2/S & \Delta\tilde{x}_1/S & 0 \\ -\Delta\tilde{x}_1\Delta\tilde{x}_3/(SL) & -\Delta\tilde{x}_2\Delta\tilde{x}_3/(SL) & s/L \end{bmatrix} \begin{Bmatrix} \bar{\mathbf{e}}_1 \\ \bar{\mathbf{e}}_2 \\ \bar{\mathbf{e}}_3 \end{Bmatrix} \tag{53}$$

where $S = \left(\Delta\tilde{x}_1^2 + \Delta\tilde{x}_2^2\right)^{\frac{1}{2}}$.
Thus we can define a transformation matrix $\tilde{\boldsymbol{\lambda}}_0$ between $\tilde{\mathbf{e}}_i$ and $\bar{\mathbf{e}}_i$ as

$$\tilde{\boldsymbol{\lambda}}_0 = \begin{bmatrix} \Delta\tilde{x}_1/L & \Delta\tilde{x}_2/L & \Delta\tilde{x}_3/L \\ -\Delta\tilde{x}_2/S & \Delta\tilde{x}_1/S & 0 \\ -\Delta\tilde{x}_1\Delta\tilde{x}_3/(SL) & -\Delta\tilde{x}_2\Delta\tilde{x}_3/(SL) & S/L \end{bmatrix} \tag{54}$$

When the element is parallel to the $\bar{x}_3$ axis, $S = \left[\Delta\tilde{x}_1^2 + \Delta\tilde{x}_2^2\right]^{\frac{1}{2}} = 0$ and Eq.(53) is not valid. In this case, the local coordinates is determined by

$$\tilde{\mathbf{e}}_1 = \bar{\mathbf{e}}_3, \tilde{\mathbf{e}}_2 = \bar{\mathbf{e}}_2, \tilde{\mathbf{e}}_3 = -\bar{\mathbf{e}}_1 \tag{55}$$

Let x_i and $\mathbf{e}_i$ be the co-rotational reference coordinates for the deformed rod element. In order to continuously define the local coordinates of the same rod element during the whole range of large deformation, the basis vectors $\mathbf{e}_i$ are chosen such that

$$\begin{aligned}
\mathbf{e}_1 &= (\Delta x_1\bar{\mathbf{e}}_1 + \Delta x_2\bar{\mathbf{e}}_2 + \Delta x_3\bar{\mathbf{e}}_3)/l = a_1\bar{\mathbf{e}}_1 + a_2\bar{\mathbf{e}}_2 + a_3\bar{\mathbf{e}}_3 \\
\mathbf{e}_2 &= (\tilde{\mathbf{e}}_3 \times \mathbf{e}_1)/|\tilde{\mathbf{e}}_3 \times \mathbf{e}_1| \\
\mathbf{e}_3 &= \mathbf{e}_1 \times \mathbf{e}_2
\end{aligned} \tag{56}$$

where $\Delta x_i = x_i^2 - x_i^1, l = \left(\Delta x_1^2 + \Delta x_2^2 + \Delta x_3^2\right)^{\frac{1}{2}}$.
We denote $\tilde{\mathbf{e}}_3$ in Eq.(53) as

$$\tilde{\mathbf{e}}_3 = c_1\bar{\mathbf{e}}_1 + c_2\bar{\mathbf{e}}_2 + c_3\bar{\mathbf{e}}_3 \tag{57}$$

Then $\mathbf{e}_i$ and $\bar{\mathbf{e}}_i$ have the following relations:

$$\begin{Bmatrix} \mathbf{e}_1 \\ \mathbf{e}_2 \\ \mathbf{e}_3 \end{Bmatrix} = \begin{bmatrix} a_1 & a_2 & a_3 \\ b_1 & b_2 & b_3 \\ a_2b_3 - a_3b_2 & a_3b_1 - a_1b_3 & a_1b_2 - a_2b_1 \end{bmatrix} \begin{Bmatrix} \bar{\mathbf{e}}_1 \\ \bar{\mathbf{e}}_2 \\ \bar{\mathbf{e}}_3 \end{Bmatrix} = \boldsymbol{\lambda}_0 \bar{\mathbf{e}}_i \tag{58}$$

where

$$\begin{aligned} b_1 &= (c_2a_3 - c_3a_2)/l_{31} \\ b_2 &= (c_3a_1 - c_1a_3)/l_{31} \\ b_3 &= (c_1a_2 - c_2a_1)/l_{31} \end{aligned} \tag{59}$$

$$l_{31} = \left[(c_2a_3 - c_3a_2)^2 + (c_3a_1 - c_1a_3)^2 + (c_1a_2 - c_2a_1)^2 \right]^{\frac{1}{2}} \tag{60}$$

and

$$\boldsymbol{\lambda}_0 = \begin{bmatrix} a_1 & a_2 & a_3 \\ b_1 & b_2 & b_3 \\ a_2b_3 - a_3b_2 & a_3b_1 - a_1b_3 & a_1b_2 - a_2b_1 \end{bmatrix} \tag{61}$$

Thus, the transformation matrix $\boldsymbol{\lambda}$, between the 12 generalized coordinates in the co-rotational reference frame, and the corresponding 12 coordinates in the global Cartesian reference frame, is given by

$$\boldsymbol{\lambda} = \begin{bmatrix} \boldsymbol{\lambda}_0 & & & \\ & \boldsymbol{\lambda}_0 & & \\ & & \boldsymbol{\lambda}_0 & \\ & & & \boldsymbol{\lambda}_0 \end{bmatrix} \tag{62}$$

Letting x_i and $\mathbf{e}_i$ be the reference coordinates, and repeating the above steps [Eq.(56) – Eq.(62)], the transformation matrix of each incremental step can be obtained in a same way.

Then the element matrices are transformed to the global coordinate system using

$$\bar{\mathbf{a}}^k = \boldsymbol{\lambda}^T \hat{\mathbf{a}}^k \tag{63}$$

$$\bar{\mathbf{K}}^k = \boldsymbol{\lambda}^T \hat{\mathbf{K}}^k \boldsymbol{\lambda} \tag{64}$$

$$\bar{\mathbf{F}}^k = \boldsymbol{\lambda}^T \hat{\mathbf{F}}^k \tag{65}$$

where $\bar{\mathbf{a}}^k, \bar{\mathbf{K}}^k, \bar{\mathbf{F}}^k$ are respectively the generalized nodal displacements, element tangent stiffness matrix and generalized nodal forces, in the global coordinates system.

After assembling the element stiffness matrices and nodal force vectors, into their global counterparts, we obtain the discretized equations of the space frames as

$$\mathbf{Ka} = \mathbf{F}^{1} - \mathbf{F}^{S0} \tag{66}$$

The Newton-Raphson method, modified Newton-Rapson method or the artificial time integration method (Liu 2007a, 2007b; Liu and Atluri 2008) can be employed to solve Eq.(66). In this implementation, the Newton-Raphson algorithm is used. The iterative Newton-Raphson procedures for Eq.(66) is given as

$$\mathbf{K}^{m}\mathbf{a}^{m} = \mathbf{F}^{1} - \mathbf{F}^{S(m)} \tag{67}$$

where

$$\mathbf{F}^{S(m)} = \int_{l} \mathbf{B}_{L}^{T} \boldsymbol{\sigma}^{1(m)} dl \tag{68}$$

$$\bar{\mathbf{u}}^{m+1} = \bar{\mathbf{u}}^{m} + \mathbf{a}^{m} \tag{69}$$

and $\bar{\mathbf{u}}$ are the total displacements in global coordinates.

5 Numerical examples

5.1 Buckling of a beam

The (12×12) tangent stiffness matrix for a beam in space should be capable of predicting buckling under compressive axial loads, when such an axial load interacts with the transverse displacement in the beam. We consider a simply supported beam subject to an axial force as shown in Fig.4 and assume that $EI = 1$ and $L = 1$. The buckling loads of the beam obtained by the present method using different numbers of elements are shown in Tab.1. It is seen that the buckling load predicted by the present method agrees excellently with the analytical solution (buckling load is π^2).

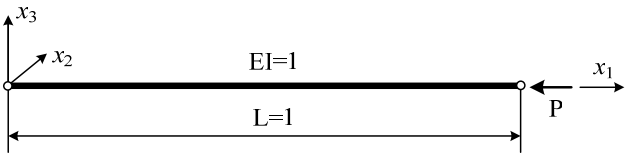

Figure 4: A simply supported beam subject to an axial force

Table 1: Buckling load of the simply supported beam

	Present method(Number of elements)					Analytical solution
	1	2	3	4	5	
Buckling load	12.005	9.940	9.881	9.872	9.872	9.870

When the beam is fixed at $x_1 = 0$, while at the other end it is free and under a compressive load P, the buckling load of the beam obtained by the present method using different number of elements is shown in Tab.2 (the analytical solution is $\frac{\pi^2 EI}{4L^2}$).

Table 2: Buckling load of the beam fixed at $x_1 = 0$

	Present method(Number of elements)					Analytical solution
	1	2	3	4	5	
Buckling load	2.4860	2.4687	2.4677	2.4675	2.4674	2.4674

5.2 Large deformation analysis of a cantilever beam with a symmetric cross section

A large deflection and moderate rotation analysis of a cantilever beam subject to a transverse load at the tip, as shown in Fig. 5, is considered. The cross section of the beam is a square with $h = 1$. The Poisson's ration is $\nu = 0.3$. Fig.6 shows the results obtained in the analysis of the cantilever problem. It is seen that the present results using 10 elements agree excellently with those of Bathe and Bolourchi (1979).

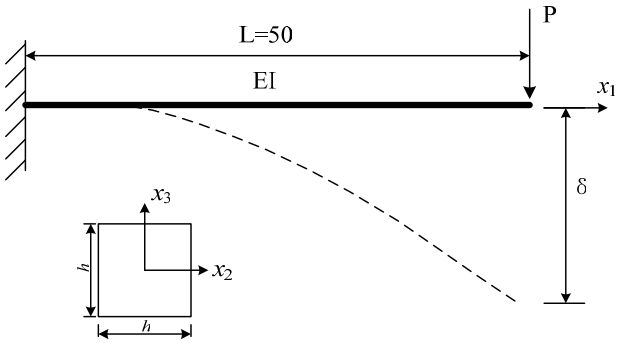

Figure 5: A cantilever beam subject to a transverse load at the tip

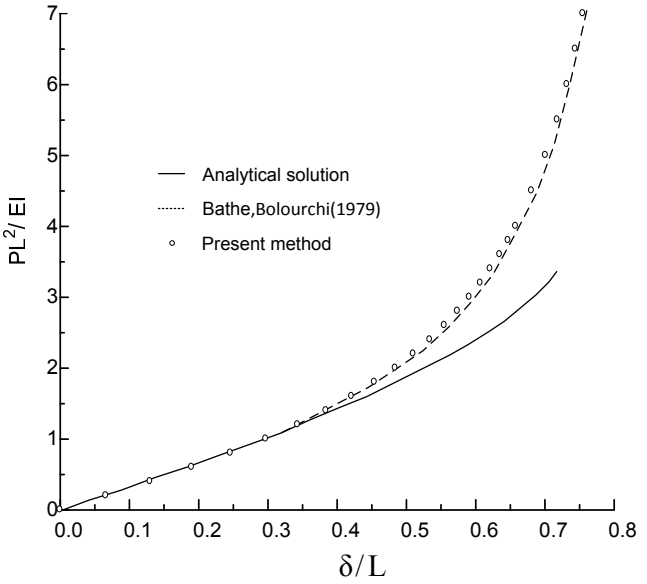

Figure 6: Deflections of a cantilever under a concentrated load

5.3 Large rotations of a cantilever subject to an end-moment and a transverse load

An initially-straight cantilever subject to an end moment $M^* = \frac{ML}{2\pi EI}$ (Crisfield 1990) as shown in Fig.7, is considered. The beam is divided into 10 equal elements. When $M^* = 1$, the beam is curled into a complete circle as shown in Fig.7.

If a non-conservative, follower-type transverse load $P^* = \frac{PL^2}{2\pi EI}$ is applied at the tip, instead of M^*, the initial and deformed geometries of the cantilever are shown in Fig.8. It should be pointed out that the solution was found to diverge when using the explicit tangent stiffness of the present paper when $P^* > 4.5$. However, when the exact integration in Eq.(44) was used, the solution was found to converge.

5.4 Large deformation analysis of a cantilever beam with an asymmetric cross section

We consider the large deflection of a cantilever beam with an asymmetric cross section, as shown in Fig.9. The Poisson's ration is $\nu = 0.3$. The areas of the symmetric and asymmetric cross section in Fig.9 are all equal to 1.

Fig.10 shows the comparison of the deflections in x_3 direction, between the cases

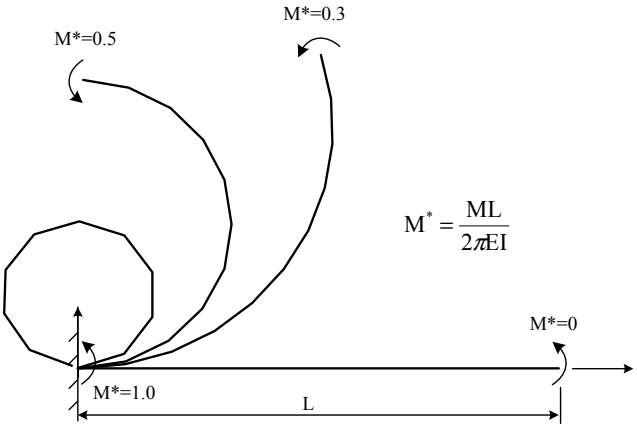

Figure 7: Initial and deformed geometries for cantilever subject to an end-moment

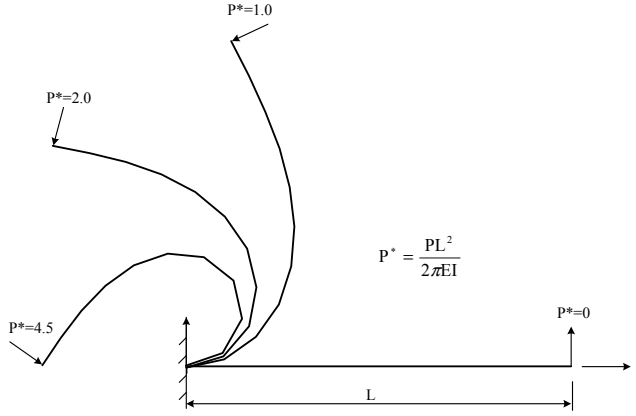

Figure 8: Initial and deformed geometries for cantilever subject to a transverse load

of symmetric and asymmetric cross sections. Fig.11 shows the deflection in x_2 direction for the cantilever beam with an asymmetric cross section. However, the deflections in x_2 direction are zero in the case of a symmetric cross section.

5.5 Large displacement analysis of a 45-degree space bend

The large displacement response of a 45-degree bend subject to a concentrated end load [Bathe and Bolourchi (1979)] is calculated as shown in Fig.12. The radius of the bend is 100, the cross section area is 1 and lies in the $x_1 - x_2$ plane. The concentrated is applied in the x_3 direction.

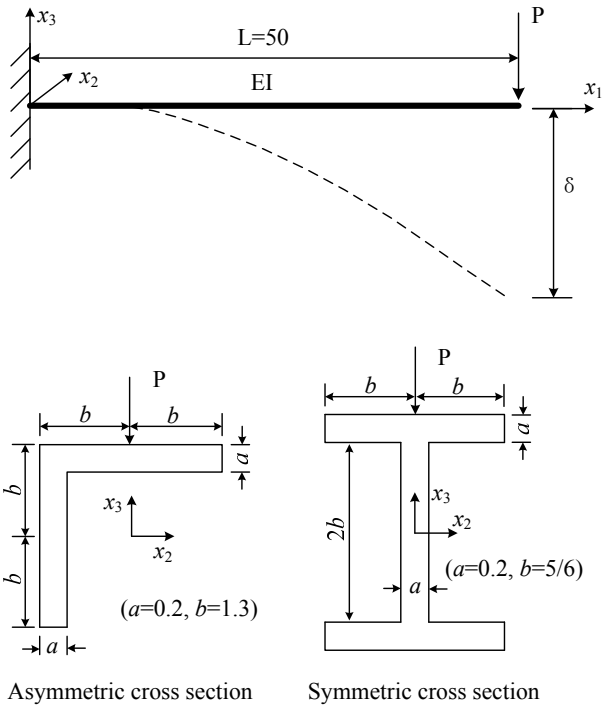

Figure 9: A cantilever beam with an asymmetric cross section

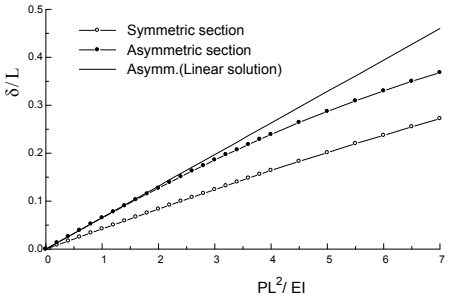

Figure 10: Comparison of the deflections in x_3 direction of a cantilever beam

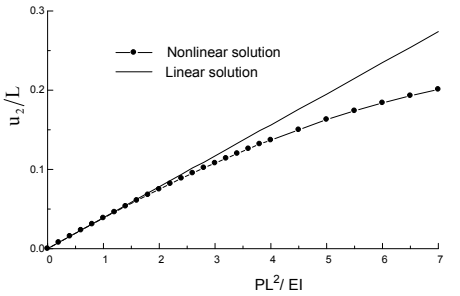

Figure 11: Deflections in x_2 direction for the cantilever beam with asymmetric cross section

8 equal straight elements and 140 equal load steps are used in the analysis of the problem. Fig.13 shows the tip deflection predicted by the present method and Bathe and Bolourchi (1979). It can be seen that the results of the present method are

comparable to the results of Bathe and Bolourchi (1979) even when the simplified rod theory is adopted as in the present implementation.

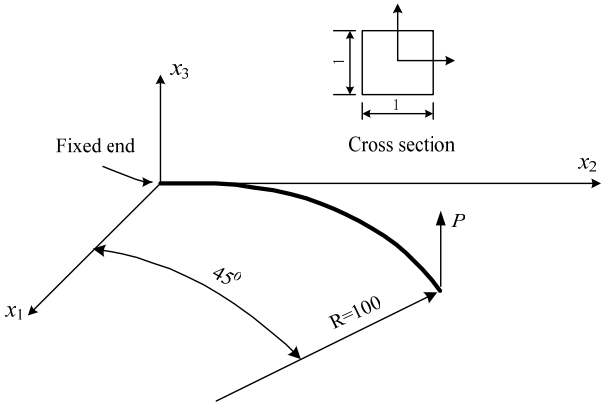

Figure 12: Model of a 45-degree circular bend

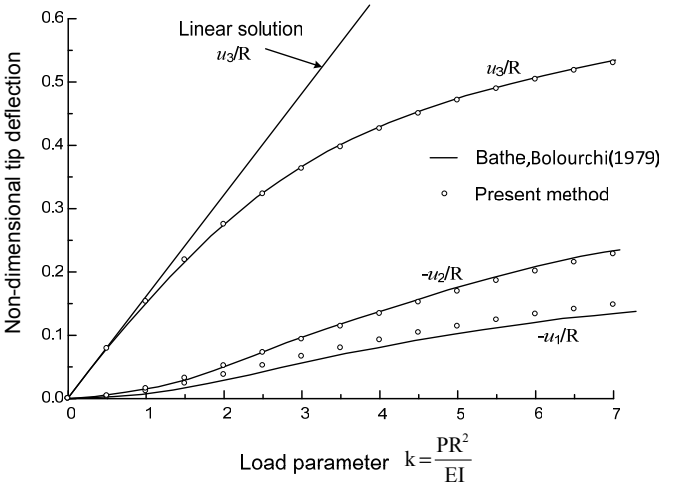

Figure 13: Three-dimensional large deformation of a 45-degree circular bend

5.6 A framed dome

A framed dome shown in Fig.14 is considered (Shi and Atluri 1988). A concentrated vertical load P is applied at the crown point. Each member of the dome is

modeled by 4 elements. The force-displacement curve at the crown point is shown in Fig.15. It is seen that the present results agree well with the results of Kondoh, Tanaka and Atluri (1986), and Shi and Altluri (1988).

It should be mentioned here that it is sufficient to use a single element to model each member of the space frame if we use numerical integration in Eq.(45) instead of assuming that σ_1^k is constant in a rod element.

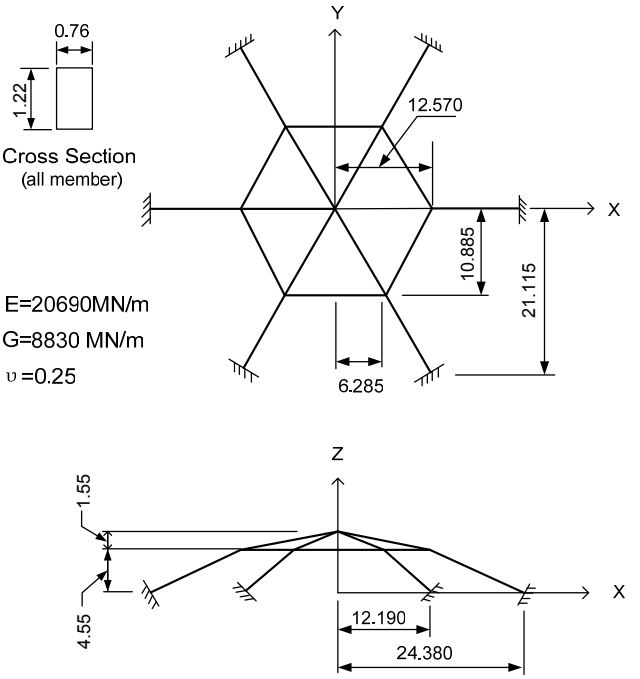

Figure 14: Framed dome (the unit of length is metre)

6 Conclusions

Based on a von Karman type nonlinear theory in a rotated reference frame, a simplified finite deformation theory of a cylindrical rod subjected to bending and torsion has been developed, and a simple and economic element for large deformation analysis of space frames has been successfully implemented. The proposed method is capable of handling large rotation geometrically nonlinear analysis of frames with arbitrary cross sections, which haven't been considered by a majority of previous studies. It is shown to be possible to derive an explicit expression for the tangent stiffness matrix of each element even if assumed-displacement type formulations

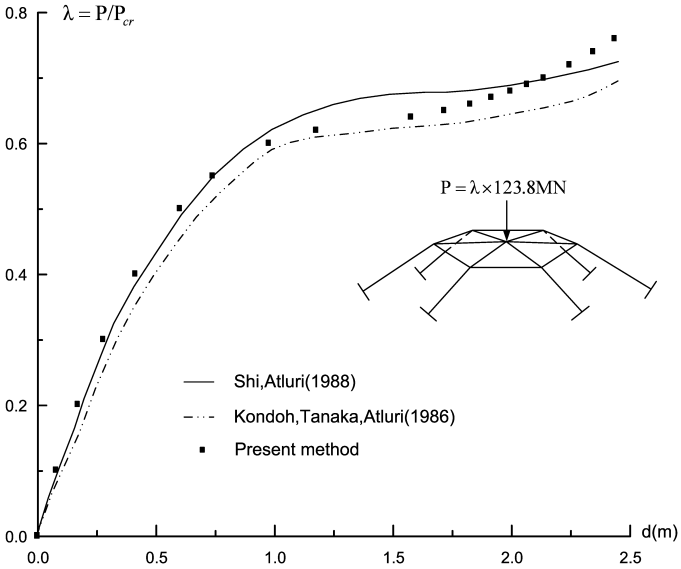

Figure 15: Force-displacement curve for the crown point of a framed dome

are used. Numerical examples demonstrate that the present method is just as competitive as the existing methods in terms of accuracy and efficiency. The present method can be extended to consider the formation of plastic hinges in each beam of the frame; and also to consider large-rotations of plates and shells, by implementing only a von Karman type nonlinear theory in the co-rotational reference frame of each beam/plate element.

Acknowledgement: The authors gratefully acknowledge the support of the Nature Science Foundation of China (NSFC, 10972161). This research was also supported by the World Class University (WCU) program through the National Research Foundation of Korea funded by the Ministry of Education, Science and Technology (Grant no.: R33-10049). The second author is also pleased to acknowledge the support of the Lloyd's Register Educational Trust (LRET) which is an independent charity working to achieve advances in transportation, science, engineering and technology education, training and research worldwide for the benefit of all.

References

Atluri, S.N. (1980): On some new general and complementary energy theorems for the rate problems in finite strain, classical elastoplasticity. *Journal of Structural*

Mechanics, Vol. 8(1), pp. 61-92.

Atluri, S.N. (1984): Alternate stress and conjugate strain measures, and mixed variational formulations involving rigid rotations, for computational analyses of finitely deformed plates and shells: part-I: thoery. *Computers & Structures*, Vol. 18(1), pp. 93-116.

Atluri, S.N.; Cazzani, A. (1994): Rotations in computational solid mechanics, invited feature article. *Archives for Computational Methods in Engg*., ICNME, Barcelona, Spain, Vol 2(1), pp. 49-138.

Atluri, S.N.; Iura, M.; Vasudevan, S. (2001): A consistent theory of finite stretches and finite rotations, in space-curved beams of arbitrary cross-section. *Computational Mechanics*, vol.27, pp.271-281

Auricchio, F.; Carotenuto, P.; Reali,A. (2008): On the geometrically exact beam model: A consistent, effective and simple derivation from three-dimensional finite-elasticity. *International Journal of Solids and Structures*, vol.45, pp. 4766–4781.

Bathe, K.J.; Bolourchi, S. (1979): Large displacement analysis of three- dimensional beam structures. *International Journal for Numerical Methods in Engineering,* vol.14, pp.961-986.

Chan, S.L. (1996): Large deflection dynamic analysis of space frames. *Computers & Structures*, vol. 58, pp.381-387.

Crisfield, M.A. (1990): A consistent co-rotational formulation for non-linear, three-dimensional, beam-elements. *Computer Methods in Applied Mechanics and Engineering*, vol.81, pp. 131–150.

Dinis, L.W.J.S.; Jorge, R.M.N.; Belinha, J. (2009): Large deformation applications with the radial natural neighbours interpolators. *CMES: Computer Modeling in Engineering & Sciences*, vol.44, pp. 1-34

Gendy, A.S.; Saleeb, A.F. (1992): On the finite element analysis of the spatial response of curved beams with arbitrary thin-walled sections. *Computers & Structures*, vol.44, pp.639-652

Han, Z.D.; Rajendran, A.M.; Atluri, S.N. (2005): Meshless Local Petrov- Galerkin (MLPG) approaches for solving nonlinear problems with large deformations and rotations. *CMES: Computer Modeling in Engineering & Sciences*, vol.10, pp. 1-12

Iura, M.; Atluri, S.N. (1988): Dynamic analysis of finitely stretched and rotated 3-dimensional space-curved beams. *Computers & Structures*, Vol. 29, pp.875-889

Izzuddin, B.A. (2001): Conceptual issues in geometrically nonlinear analysis of 3D framed structures. *Computer Methods in Applied Mechanics and Engineering*, vol.191, pp. 1029–1053.

Kondoh, K.; Tanaka, K.; Atluri, S.N. (1986): An explict expression for the

tangent-stiffness of a finitely deformed 3-D beam and its use in the analysis of space frames. *Computers & Structures*, vol.24, pp.253-271.

Kondoh, K.; Atluri, S.N. (1987): Large-deformation, elasto-plastic analysis of frames under nonconservative loading, using explicitly derived tangent stiffnesses based on assumed stresses. *Computational Mechanics*, vol.2,pp.1-25.

Lee, M.H.; Chen, W.H. (2009): A three-dimensional meshless scheme with background grid for electrostatic-structural analysis. *CMC: Computers Materials & Continua*, vol.11, pp. 59-77

Lee, S.Y.; Lin, S.M.; Lee, C.S.; Lu, S.Y.; Liu, Y.T. (2008): Exact large deflection of beams with nonlinear boundary conditions. *CMES: Computer Modeling in Engineering & Sciences*, vol.30, pp. 27-36

Lee, S.Y.; Lu, S.Y.; Liu, Y.R.; Huang, H.C. (2008): Exact large deflection solutions for Timoshenko beams with nonlinear boundary conditions. *CMES: Computer Modeling in Engineering & Sciences*, vol.33, pp. 293-312

Liu, C.S. (2007a): A modified Trefftz method for two-dimensional Laplace equation considering the domain's characteristic length. *CMES: Computer Modeling in Engineering & Sciences*, vol. 21, pp. 53-66.

Liu, C.S. (2007b): A highly accurate solver for the mixed-boundary potential problem and singular problem in arbitrary plane domain. *CMES: Computer Modeling in Engineering & Sciences*, vol. 20, pp. 111-122.

Liu, C.S.; Atluri, S.N. (2008): A novel time integration method for solving a large system of non-linear algebraic equations. *CMES:Computer Modeling in Engineering & Sciences*, vol.31, pp. 71-83.

Lo, S.H. (1992): Geometrically nonlinear formulation of 3D finite strain beam element with large rotations. *Computers & Structures*, vol.44, pp.147-157

Mata, P.; Oller, S.; Barbat A.H. (2007): Static analysis of beam structures under nonlinear geometric and constitutive behavior. *Computer Methods in Applied Mechanics and Engineering*, vol.196, pp. 4458–4478.

Mata, P.; Oller, S.; Barbat A.H. (2008): Dynamic analysis of beam structures considering geometric and constitutive nonlinearity. *Computer Methods in Applied Mechanics and Engineering*, vol.197, pp. 857–878.

Punch, E.F.; Atluri, S.N. (1984): Development and testing of stable, invariant, isoparametric curvilinear 2-D and 3-D hybrid-stress elements. *Computer Methods in Applied Mechanics and Engineering* ,Vol.47, pp.331-356

Simo, J.C. (1985): A finite strain beam formulation. The three-dimensional dynamic problem. Part I. *Computer Methods in Applied Mechanics and Engineering*, vol. 49, pp.55–70.

Shi, G.; Atluri, S.N. (1988): Elasto-plastic large deformation analysis of space-frames: a plastic-hinge and strss-based explict derivation of tangent stiffnesses. *International Journal for Numerical Methods in Engineering*, vol.26, pp.589-615.

Wu, T.Y.; Tsai, W.G.;Lee, J.J. (2009): Dynamic elastic-plastic and large deflection analyses of frame structures using motion analysis of structures. *Thin-Walled Structures*, vol.47, pp. 1177- 1190.

Xue, Q.; Meek J.L. (2001): Dynamic response and instablity of frame structures. *Computer Methods in Applied Mechanics and Engineering*, vol.190, pp. 5233–5242.

Zhou, Z.H.; Chan,S.L. (2004a): Elastoplastic and Large Deflection Analysis of Steel Frames by One Element per Member. I: One Hinge along Member. *Journal of Structural Engineering*, vol. 130, pp.538–544.

Zhou, Z.H.; Chan,S.L. (2004b): Elastoplastic and Large Deflection Analysis of Steel Frames by One Element per Member. II: Three Hinges along Member. *Journal of Structural Engineering*, vol. 130, pp.545–5553.